Evaluation of rainfall estimation derived from commercial interactive DVB receivers using disdrometer, rain gauge, and weather radar

Elisa Adirosi, Luca Facheris, Filippo Giannetti, Simone Scarfone, Giacomo Bacci, *Member IEEE*,
Alessandro Mazza, Alberto Ortolani and Luca Baldini, *Senior Member IEEE*

Abstract—**Accurate measurement and monitoring of precipitation is crucial for many applications, such as flood and drought risk assessment and management. Conventional meteorological devices for estimating precipitation (i.e. rain gauges, disdrometers, active and passive remote sensors, be they ground based, spaceborne or airborne) have their own strengths and weaknesses. The latter are often related to time and space resolution, coverage, and cost. In the last two decades, several studies have been carried out to exploit opportunistic signals of terrestrial microwave communication links to improve precipitation estimation capability. This study describes and evaluates a method to retrieve rainfall rate from the signal-to-noise ratio obtained from commercial interactive digital video broadcasting (DVB) receivers (referred as to smartLNBs). During a 1-year measurement campaign carried out in Tuscany (Italy) with purposely deployed instruments, the precipitation values estimated from a set of SmartLNBs were compared with measurements from co-located rain gauges and disdrometer. The normalized mean absolute error (NMAE) and root mean square error (RMSE) obtained comparing the total cumulative precipitation from a SmartLNB and a disdrometer are 48.8% and 7.46 mm, respectively. Encouraging results also come from comparing the total precipitation amounts as measured by the SmartLNBs and by the rain gauges, with values of NMAE (respectively, RMSE) ranging between 44% and 82% (respectively, 5.2 mm and 11.5 mm).**

Index Terms—**Rainfall rate estimation, satellite-to-ground links, signal of opportunity**

I. INTRODUCTION

PRECIPITATION is closely related to different aspects of human life. Its accurate measurement is crucial for many applications, such as management of water resources, prediction of wildfire risk, floods, and landslides. To date, quantitative precipitation estimation can be obtained by several observing systems using different measurement principles that have different time and space resolutions, and accuracies [1]. Historically, rain gauges were the first devices adopted to measure the rainfall accumulated (in mm) in a given amount of time and at given location. Their measurements are considered accurate, although differences in the performance of instruments produced by different manufacturers and with different characteristics were documented [2]. They are point devices with a small measuring area. To provide maps of the spatial distribution of the cumulated rainfall, weather and hydrology services use networks of telemetered rain gauges, which are usually characterized by a spatially

Fig. 1. Main components of the NEFOCAST satellite network.

inhomogeneous density [3]. The spatial accuracy of such rainfall maps is usually low and highly dependent on the distribution and density of the devices within the area of interest. More recently, other point-measurement instruments of the non-catching type, called *disdrometers* have been introduced to provide estimates of the drop size distribution (DSD) and drop fall velocity, from which the corresponding rainfall rate in mm h^{-1} [4] can be computed. These are still considered research devices as they are typically used in dedicated field campaigns or for specific research investigations, and are less common than rain gauges. Remote sensing devices (such as spaceborne or airborne passive or active sensors, and ground-based weather radars) provide indirect measurements of precipitation requiring appropriate retrieval algorithms. Quantitative precipitation estimation (QPE) from satellite sensors, both active and passive, is available on a global scale [5] but suffers from scarce time and space resolution, whereas ground based weather radars have a higher temporal (from 5 to 10 min) and spatial resolution (less than 1 km, although not uniform). Although most developed countries manage a weather radar network, there are regions of the globe where such networks are not available (e.g., see http://wrd.mgm.gov.tr for availability and distribution of operational weather radars over the Earth). In some regions of the world, there is a scarce availability even of rain gauges [6].

In the last few decades, the use of opportunistic microwave (MW) communication links has been investigated to retrieve, in general, weather information, and, in particular, to provide precipitation estimates. The basic idea is to estimate precipitation relying on the attenuation of the signal along the MW link caused by the presence of precipitation along the propagation path. As is well known, an electromagnetic (e.m.) wave that propagates in the atmosphere interacts with its components (i.e. gases, clouds and precipitation particles) and - depending on the wavelength - may result to be attenuated due to both scattering and absorption phenomena. At the frequencies of interest for this paper, namely the Ku band (10-12 GHz), attenuation is significant, caused by the interaction of the e.m. wave with liquid and mixed phase hydrometeors [7]. In rainfall, the specific attenuation (k, in dB km^{-1}) is linked to the rainfall rate (R, in mm h^{-1}) through a power law of the kind $k=aR^b$ (referred to as k-R relation), whose coefficients depend on frequency, polarization, temperature, particle types, and size distribution of cloud and precipitation particles. A specific ITU recommendation [8] provides the coefficients of the k-R relation for different polarization types and frequencies, with the aim to designing reliable communication systems. However, the k-R coefficients can be also obtained from measured sets of DSDs. In particular, the use of long time series of measured DSDs would provide relations that are more representative of the climate of the geographic area where the measurements were collected.

Using MW links of cellular communication networks to estimate precipitation has been the subject of several studies aiming also to demonstrate the possibility to obtain rainfall maps in areas where traditional rainfall measurement devices are scarce (see the review in [9] and references therein). Some recent studies aimed to investigate the use of attenuation measurements made along satellite-to-ground links of communication satellites in order to estimate precipitation. Comparing rainfall estimates obtained from attenuation estimated by Ku-band satellite receivers and a C-band ground-based weather radar, a discrepancy of less than 15% was found for the total amount of rainfall collected in 1-3 hour events, while higher discrepancies were found for very short and long-lasting events [10]. In a more recent experiment, rainfall rate was retrieved from signals collected from a Ku-band geostationary satellite using a receiving apparatus based on a low-noise block (LNB) receiver and analyzed with a signal meter and a network analyzer. Estimates were compared with the ones of a ground-based radar of the U.S. Next Generation Weather Radar (NEXRAD) network. A difference of up to 53% between satellite- and radar-based estimates of 24h cumulated rainfall was found [11]. In Italy, similar results were found using specifically built receivers and calibrated rain gauges for validation [12].

The Italian project NEFOCAST, funded by the Government of the Tuscany Region (Italy), has been recently carried out and concluded. The objective was to estimate rainfall rate based on attenuation measurements made by a widespread network of a new-generation of commercially available interactive digital video broadcasting (DVB) receivers, called SmartLNBs (Smart Low-Noise Block converter), developed with the aim of replacing the traditional direct-to-home receivers. Such domestic terminals, intended for interactive satellite services, can be employed as opportunity weather sensors. In fact, they have the intrinsic capability of measuring the attenuation experienced by the downlink signal and relaying it on an auxiliary return channel. They do not require any additional equipment for analyzing the received signal and can autonomously transmit weather data for further processing. In particular, the SmartLNBs are able to collect attenuation data and make them available to a dedicated platform, the NEFOCAST Service Center (NSC), where data are stored, processed, and shared with potential value-added service providers, as sketched in Fig. 1. In densely populated areas, these (or similar) interactive terminals could be sufficiently numerous to provide rainfall retrievals with high spatial resolution, a feature that would be added to the intrinsic

capability to provide practically continuous temporal monitoring of the phenomena. An *ad hoc* rainfall retrieval algorithm was developed, tuned and tested for these terminals [13] [14]. Within the NEFOCAST project, the SmartLNB operates at 11.3458 GHz for the forward link and at 14.2166 GHz for the return link using Eutelsat 10A geostationary broadcast satellite, located at 10°E. More technical details can be found in [13].

To validate the rain estimation algorithm, a measurement campaign of 1 year was carried out to compare the SmartLNB precipitation estimates with the measurements collected by conventional rain measuring devices. The NEFOCAST experiments are among the first ones worldwide attempting to use existing commercial DVB-S/S2 receivers, avoiding the use of dedicated hardware, to retrieve precipitation and to systematically evaluate the obtained estimates. In addition to that, the NEFOCAST system has introduced some novelties with respect to the state-of-the-art, such as the use of measured DSDs for the definition of the coefficients of the *k-R* relation and the use of forecast melting layer heights, as detailed in Section III.
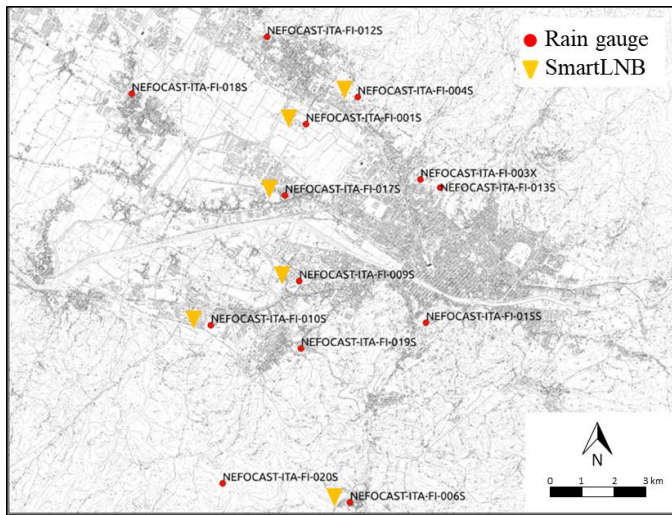

Fig. 2. Locations of smartLNBs and rain gauges of the NEFOCAST validation network in Florence.

This paper reports the main NEFOCAST findings and is organized as follow. Section II describes the experimental deployment and the meteorological devices used in the NEFOCAST field campaign. Section III describes the rain retrieval algorithm highlighting its novelty with respect to the state-of-the-art. Section IV evaluates and quantifies the intrinsic errors of the proposed algorithm, while Section V presents and discusses the main results obtained comparing the SmartLNB based estimates with the conventional meteorological devices. Finally, in Section VI the main findings are summarized and commented, pointing out the potential of the proposed technique.

II. EXPERIMENTAL DATASETS

The experimentation of the NEFOCAST system was mainly carried out within the metropolitan area of Florence (Italy) that extends over 200 km^2. The purposely deployed Validation Network (VN) consisted of 12 sites (see Fig. 2), in each of which a SmartLNB terminal produced by AYECKA Ltd. (www.ayecka.com) was installed. These terminals provide every minute the instantaneous value of the signal-to-noise ratio (defined as specified in Section III-A). Six of these sites hosted also a tipping bucket rain gauge. Each tip corresponds to an amount of water equivalent to 0.2 mm of rainfall. The time stamps of each tip are registered in a data logger and sent to the NSC using the satellite link provided by the SmartLNB.

The layout of the VN was designed to provide a joint measure by several SmartLNBs of the same precipitative event. In the metropolitan area of Florence, the elevation angle of the SmartLNB antenna with respect to the horizontal plane is practically the same for all the measurement sites and is θ_e=39.6. For what concerns the azimuthal direction (the projection of the satellite-receiver signal on the ground), it can be considered the same for all the sites, given their small mutual distance with respect to their distance from the Equator. This direction is approximately North-South as the longitude of the site area is about 11.20° East, while the satellite is in a geostationary orbit at 10° East longitude. The observation points were placed approximately along on a series of segments lined up with the North-South direction [14]. Table I describes the instrumentation installed at each site, as well as the geographical coordinates.

In addition to the VN, other SmartLNBs were installed at different locations to support the development of the rain retrieval algorithm. For instance, a SmartLNB was installed at the Dept. of Information Engineering of the University of Pisa (43.7203° N, 10.3836° E) and another one was installed on the roof of the Institute of Atmospheric Sciences and Climate (ISAC) of the National Research Council (CNR) in Rome (41.8397°N, 12.6472°E), with elevation θ_e=41.8° (higher than that used in the Florence area, since Rome is at a lower latitude). The set-up at the Rome site is shown in Fig. 3: it exploits the synergy of a

SmartLNB, a disdrometer and a C-band dual-polarization weather radar. To summarize, the data collected in Florence have been used to validate the algorithm, the data collected at University of Pisa have been mainly used to test and tune the algorithm, while the data collected at ISAC-CNR have been used to identify and evaluate he impact of the main sources of errors on the NEFOCAST algorithm and to further validate the algorithm with disdrometer data.

The disdrometer on the roof of ISAC-CNR in Rome is a laser-based Thies Clima (TC) optical device manufactured by Adolf Thies GmbH & Co. (www.thiesclima.com), Germany.

TABLE I
INSTRUMENTATION AT THE SITES OF THE NEFOCAST VALIDATION NETWORK

	Lat (deg)	Lon (deg)	Instrumentation
NEFOCAST-ITA-FI012S	43.8431	11.1863	SmartLNB
NEFOCAST-ITA-FI001S	43.8177	11.2008	SmartLNB, Rain Gauge
NEFOCAST-ITA-FI017S	43.7974	11.1917	SmartLNB, Rain Gauge
NEFOCAST-ITA-FI018S	43.8278	11.1322	SmartLNB
NEFOCAST-ITA-FI019S	43.7534	11.1964	SmartLNB
NEFOCAST-ITA-FI004S	43.8251	11.2215	SmartLNB, Rain Gauge
NEFOCAST-ITA-FI009S	43.7728	11.1964	SmartLNB, Rain Gauge
NEFOCAST-ITA-FI013S	43.7985	11.2532	SmartLNB
NEFOCAST-ITA-FI015S	43.7598	11.2461	SmartLNB
NEFOCAST-ITA-FI010S	43.7607	11.1611	SmartLNB, Rain Gauge
NEFOCAST-ITA-FI020S	43.7152	11.1641	SmartLNB
NEFOCAST-ITA-FI006S	43.7088	11.2142	SmartLNB, Rain Gauge

Every minute, TC records the number of particles that fall through its detection area of 46.5 cm^2 in a 22 (sizes) × 20 (fall velocities) matrix. The particle diameter classes range between 0.125 mm and 8 mm, while the fall velocity ranges between 0.2 m s^{-1} and 10 m s^{-1}. Knowing the drop count matrix, the DSD can be computed as

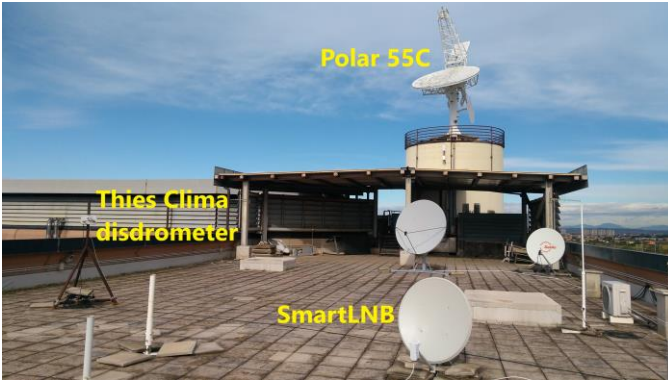$$N(D_i) = \frac{1}{A \, \Delta D_i \, \Delta t \, v_i} \sum_{j=1}^{20} n_{i,j} \qquad (1)$$

Fig. 3. NEFOCAST set up at CNR-ISAC in Rome

where A is the measuring area (m^2), ΔD is the diameter class width (mm), Δt is the time interval set equal to 60 s, $n_{i,j}$ is the number of particles detected in the i-th diameter class and j-th fall velocity class, and v_i is the fall velocity computed with the relation in [15]. Please note that, although the TC provides an estimate of the fall velocity, a theoretical relationship between the terminal fall velocity and the drop diameter is adopted for DSD computation. The latter is a common practice when DSD is used to estimate rainfall parameters because the measured fall speed may be biased due to the presence of up/down draft and is more affected by instrumental error. Before computing the DSD, a filter criterion is adopted: the drops with measured velocities outside ±50% of the [15] fall velocity are discarded. This well consolidated procedure in disdrometer-related studies (see [16] and references therein) allows to filter out the so-called spurious drops (such as the ones due to splashing and wind effects), mitigating the errors due to environmental factors. A comparing performance analysis involving the TC and other types of disdrometer can be found in [17] and references therein. The Polar 55C installed on the top of the roof of ISAC-CNR building in Rome is a research grade Doppler dual polarization coherent radar that operates at C-band (5.6 GHz) [18]. During the

NEFOCAST project, it was operated in pointing mode with the same elevation angle of the SmartLNB, so that the two devices could scan the same portion of the atmosphere (see Fig. 3).

III. METHODS

A. Rain-Retrieval Algorithm Outline

The main input of the proposed rain retrieval algorithm is the radiofrequency (RF) signal-to-noise ratio (SNR) η evaluated at the receiver input and defined as the ratio between the average received power of the information-carrying signal and the power of the additive white Gaussian noise evaluated over the RF signal bandwidth[1].

In the practice, the actual values of the ratio η are not known and therefore we must resort to the raw estimates $\hat{\eta}$ that are provided by the SmartLNB receivers using a proprietary Digital Signal Processing algorithm with a resolution of 0.1 dB and sampling rate ρ. The results presented in this paper were obtained with a sampling rate of 1 sample per minute, but the SmartLNB device can support sampling rates as fast as 1 sample every 10 s. Experimental measurements carried out in Tuscany (Italy) showed that the SNR in dry conditions (i.e., without additional rain attenuation) is about 10.4 dB [2], the actual value being however affected by tropospheric scintillation noise, 24-h periodic fluctuations due to satellite orbit perturbations and other time-varying impairments. Let us notice that the SNR estimate algorithm (see e.g. [19] and the references therein) requires the prior acquisition of all the signal syncs (i.e., both symbol clock and carrier phase/ frequency). The minimum value of the SNR necessary for a proper functioning of the synchronization and data detection blocks is termed outage threshold (η_{outage}), and its actual value depends on the adopted modulation and coding scheme. The satellite link considered in this study for rain estimation, carries a digital video signal in DVB-S2 format, with Quadriphase-Shift Keying (QPSK) modulation and BCH/LDPC concatenated error correcting code with rate 4/5, which, according to the ETSI standard [20] requires a minimum SNR of about 5 dB. Thus, the estimates $\hat{\eta}$ are available as long as the operating SNR of the receiver exceeds η_{outage}. In the following, we assume perfect estimates, i.e., $\hat{\eta} = \eta$, for $\eta > \eta_{outage}$.

In the presence of rain along the propagation path, a decrease of η is expected. The procedure for the estimation of the rainfall rate based upon the measured SNR can be summarized in four steps (see [13] for more details about the Kalman-based processing):

1. a slow-response Kalman filter removes the noise from raw SNR samples during dry periods and produces the samples $\eta^{(dry)}$ which will be used during wet periods as the reference value for the measurement of the rain attenuation;

2. a fast-response Kalman filter removes the noise from raw SNR samples and produces the sequence $\eta^{(wet)}$ which, thanks to the filter settings, is capable to track the actual SNR also during the rain;

3. the attenuation $L_{rain}(t)$ of the SNR due to the rain on the satellite downlink is estimated, ;

4. the rain rate $\hat{R}(t)$ is eventually estimated from $L_{rain}(t)$.

Unfortunately, in a *real* system this procedure is affected by several time-varying impairments, which, if not adequately tackled, compromise the accuracy of the resulting estimate. These include: *i*) scintillation fading, i.e, rapid fluctuations in signal amplitude caused by small-scale irregularities in the tropospheric refractive index; *ii*) orbit perturbations due to the gravitational effects of the Moon and the Sun; *iii*) longitudinal drift of the satellite orbital position due to Earth's gravity anomalies; *iv*) beam bending caused by large-scale changes in the medium refractive index (due to the variations of atmospheric temperature, pressure, and humidity); *v*) Sun transit behind the satellite which causes short-term "blinding" of the receiver (this occurs around the equinoxes); *vi*) occasional changes of the transponder gain setting, made by the satellite operator. The next subsections provide the details of the procedure.

B. SNR in Dry Conditions

In *dry* conditions, i.e., in the absence of rain, the (unitless) SNR can be expressed as

$$[\eta(t)]^{(dry)} = \frac{\dfrac{\Phi G_R \lambda^2}{4\pi R_s}}{L_{atm} L_{cloud} k_B T_N^{(dry)}} \qquad (2)$$

where Φ is the signal power flux density (W m^{-2}) at the receiving antenna input, G_R is the receiving antenna gain (unitless), λ is the carrier wavelength (m), R_s is the symbol rate (in s^{-1}), L_{atm} is the atmospheric attenuation due to water vapor absorption and other gaseous effects (unitless), L_{cloud} is the attenuation due to clouds (unitless), k_B is the Boltzmann constant (J Hz^{-1}) and

---

[1] The SNR η can be equivalently provided in terms of the ratio E_s/N_0 measured at the ground terminal, where the numerator E_s represents the average RF received energy (measured in J) within the time interval of one information-bearing symbol and the denominator N_0 is the one-sided power spectral density of the Gaussian noise (measured in W Hz^{-1}) affecting the received signal.

[2] Numerical evaluation of the link-budget confirmed experimental findings.

$$T_N^{(\text{dry})} = \frac{T_c}{L_{atm}L_{cloud}} + T_m \left(1 - \frac{1}{L_{atm}L_{cloud}}\right) + T_g + T_{rx} \quad (3)$$

is the total noise temperature at the receiver input in dry conditions, where T_c=2.78 K, T_m=275 K, T_g=45 K, T_{rx}=13.67 K are respectively the noise temperatures of the cosmic background, of the meteorological formations (clouds, etc.), of the environment surrounding the antenna (mainly, ground) and of the receiver hardware.

Sky noise contributions T_c and T_m are constant and independent from the location of the receive station, and their values have been obtained from the literature. Ground noise has a little dependence on the satellite elevation, and thus on the location of the receive station, too, but for simplicity a single value was assumed valid for all the stations. Furthermore, all the commercially-available receivers have almost the same noise figure and temperature T_{rx}.

Both L_{atm} and L_{cloud} are assumed constant and can be numerically o btained according to the methodologies outlined in *"Annex 2 - 2.2.1.1 Earth-space paths"* of [21] and in *"Annex 1 - 3 Cloud attenuation along slant paths"* of [22], respectively, which also require the knowledge of the elevation angle θ_e at the receive location. For the elevation angle in Florence (θ_e=39.6°), L_{atm} resulted to be 0.09 dB, while as regards the cloud attenuation factor L_{cloud}, although it is a highly variable parameter depending on the type of clouds, for the sake of simplicity it has been assumed constant, also in consideration of its limited impact on the attenuation of the signal. L_{cloud} was therefore set to 0.041 dB based on the results of some experimental measurements carried out during the NEFOCAST project. Also, notice that, due to the signal impairments outlined above, the SNR is actually a time-varying quality metric of the link.

C. SNR in Wet Conditions

In *wet* conditions, i.e. in the presence of rain, the signal experiences an *additional* fast time-varying attenuation $L_{rain}(t)$ and, accordingly, the SNR in (2) becomes

$$[\eta(t)]^{(\text{wet})} = \frac{\frac{\Phi G_R \lambda^2}{4\pi R_s}}{L_{atm}L_{cloud}L_{rain}(t)k_B T_N^{(\text{wet})}(t)} \quad (4)$$

where

$$T_N^{(\text{wet})}(t) = \frac{T_c}{L_{atm}L_{cloud}L_{rain}(t)}$$
$$+ T_m \left(1 - \frac{1}{L_{atm}L_{cloud}L_{rain}(t)}\right) \quad (5)$$
$$+ T_g + T_{rx}$$

is the total noise temperature at the receiver input in wet conditions. Note that the rain attenuation and the total noise temperature are actually time-dependent. By manipulating (2) and (4), the rain attenuation can be formally expressed as

$$L_{rain}(t) = \frac{[\eta(t)]^{(\text{dry})}}{[\eta(t)]^{(\text{wet})}} (1 - \xi) + \xi \quad (6)$$

where we defined the following term (assumed constant for the sake of simplicity)

$$\xi \triangleq \frac{T_m - T_c}{L_{atm} L_{cloud} \left(T_m + T_g + T_{rx}\right)} \quad (7)$$

Computing (7) with the numerical values outlined above leads to $\xi = 0.792$ [23].

Equation (6) represents the basis used for evaluating $L_{rain}(t)$. It requires the availability of both the dry and wet SNRs at any instant t during the rain event. In practice, however, only the wet SNR is measurable during precipitation. As a consequence, only a presumed, fictitious value for the dry baseline SNR can be used in (6). The results presented in this paper are obtained by replacing the dry SNR in (6) with the latest value of the dry SNR measured before the rain onset, and keeping this value constant for the entire duration of the rainy event..

The maximum measurable attenuation with this method can be assessed letting $\eta(t)^{dry} = 10.4 \, dB$(i.e., the typical clear sky value of SNR) and $\eta(t)^{wet} = 5 \, dB$ (i.e., the minimum allowed value of SNR), yielding L_{rain}=1.85 dB. By inverting eq. (8) with the maximum value for L_{rain}, we get the maximum rain rate which can be estimated. The actual resulting value depends on the rain height, which, in turn, is related to the zero-degree isotherm height. The lowest height yields the maximum measurable rain rate. If the height is 1 km, the maximum rain rate is about 30 mm h^{-1} while for 2.5 km, the maximum rain rate reduces to about 16 mm h^{-1}.

D. Link Geometry and Model for Rain Attenuation

To evaluate the attenuation due to rain along a ground-satellite link, we make the simplified assumption of stratiform precipitation (Fig. 4), characterized by a clear separation, at the height of the 0° C isotherm, between an upper layer, hereinafter named the Ice Particles Layer (IPL), made of frozen and mostly dry particles, and the lower layers in which the ice particles melt into raindrops before reaching the ground. Significant excess attenuation of Ku band signal occurs in the lower layers, due to the presence of liquid-phase precipitation. The upper layer, denoted as Melting Layer (ML), has a variable thickness and contains a combination of melting ice and rain, while the lower one contains only rain and is referred to as Liquid Layer (LL). Furthermore we assumed a constant precipitation along the link path through ML and LL. The latter assumption implies a constant precipitation along a few kilometers path, that can be valid for stratiform precipitation, but can be argued in convective conditions. Impact of this assumption could be mitigated for example by resorting to using a spatialization algorithm with measurements from a dense network of SmartLNB as input, or additional external inputs from models or profiling instruments. However, this analysis is out of the scope of the paper. Please note that in convection the link geometry will be the same but the effect of mixing phase hydrometeors on the Earth-satellite link attenuation can be challenging to determine.

In the analytical model utilized hereafter, we used a downward-increasing vertical coordinate h (km), whose zero level was set coincident with the 0° C isotherm height with respect to the ground antenna. In such a reference system, the coordinates of the ML-LL boundary and of the ground antenna are denoted as δ_{ML} and h_0, respectively. In the LL ($\delta_{ML} < h \leq h_0$), the time-varying rainfall rate $R_{LL}(t)$ (mm h^{-1}), due only to liquid phase hydrometeors, is assumed independent of the vertical coordinate. In the ML ($0 \leq h \leq \delta_{ML}$), it is assumed that the fraction of liquid rain linearly increases from 0 at the 0 °C isotherm level to 1, so that at the ML-LL boundary the rain rate is equal to $R_{LL}(t)$. During a precipitation event, the radio signal propagates through the IPL, ML, and LL, whose contributions to the total excess attenuation are $L_{IPL}(t)$, $L_{ML}(t)$, $L_{LL}(t)$, respectively. We also assume that the specific rain attenuation $k(h;t)$ is a time-varying function of the vertical coordinate h, related to the rainfall rate $R_{LL}(h;t)$ according to the customary $k = aR^b$ power law. Recalling that the contribution to the total excess attenuation of the IPL is typically negligible, and adapting the power law to the 2-layer (i.e., ML-LL) model, the total excess attenuation (dB) for the typical wet conditions turns out to be the following function of the rainfall rate at ground $R_{LL}(t)$

$$L_{rain}(t) = \overbrace{\alpha_{ML}[R_{LL}(t)]^{\beta_{ML}}\left[\frac{\delta_{ML}}{(\beta_{ML}+1)\sin\theta_e}\right]}^{ML\ contribution} + \underbrace{\alpha_{LL}[R_{LL}(t)]^{\beta_{LL}}\left[\frac{h_0-\delta_{ML}}{\sin\theta_e}\right]}_{LL\ contribution} \tag{8}$$

where the values of the coefficients are supposed to be independent of h and are evaluated for the downlink frequency (11.3458 GHz). In the LL, we set $\alpha_{LL} = 0.0153$ and $\beta_{LL} = 1.2531$, according to the results of a massive experimental campaign in central Italy [13]. In the ML, we set $\alpha_{ML} = 0.01914$ and $\beta_{ML} = 1.1068$, as in [24]. Given a measured rain attenuation $L_{rain}(t)$, the inversion of (8) yields an estimate of $R_{LL}(t)$. Due to the transcendental nature of (8), this inversion calls for an iterative procedure or a look-up-table.

IV. EVALUATION OF THE RAIN RETRIEVAL ALGORITHM

The NEFOCAST algorithm allows to obtain every minute a value of R from the raw SmartLNB data, namely η. In this section, intrinsic errors of the NEFOCAST algorithm in the retrieval of R are identified and evaluated. Neglecting the SmartLNB measurement errors, the estimation of R can be affected by several sources of error, among which $i)$ errors in the estimation of L_{rain} from η, $ii)$ errors in the estimation of h_0 and δ_{ML}, and $iii)$ errors in the estimation of R from L_{rain} depending on the microphysical models adopted to parameterize the relation between attenuation and rainfall rate in the LL and in the ML. Thanks to the synergic use of disdrometer and radar data available at ISAC-CNR in Rome, we were able to quantify the contribution of
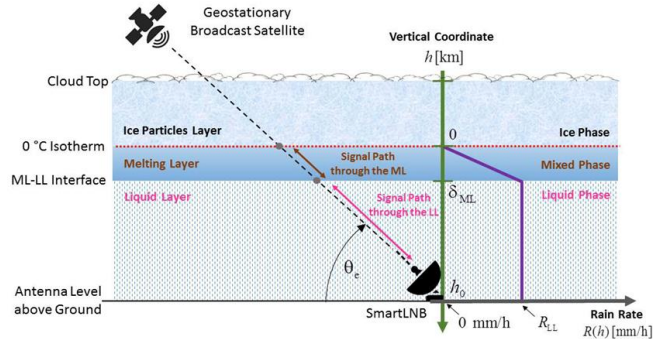

Fig. 4. Downlink geometry with stratiform rain. Violet line sketches the attenuation modelling, where R_{LL} is supposed constant in the Liquid Layer and decreases linearly in the Melting Layer until it reaches zero at the 0° isotherm [23]

ii) and *iii)* as detailed in sections IV-A and IV-B, respectively.

A. Impact of ML characteristics on retrievals

The height of the $0°$ C isotherm h_0 used un the NEFOCAST algorithm is forecasted by the numerical weather prediction (NWP) weather research and forecasting (WRF) model developed by LaMMA Consortium [13] and is made available every 6 hours, while δ_{ML} has been set constant and equal to 500 m. The use of actual values of the height and thickness of ML, instead of the predicted ones, may have an impact on the retrieved rainfall rate. Coincident disdrometer and radar measurements during 14 precipitation events, which occurred between November 2017 and January 2019 in the Rome area, were used to evaluate the effect of these two parameters on the retrieval of the rainfall rate. For each event, based on the values of equivalent reflectivity factor at horizontal polarization (Z_h, dBZ) and differential reflectivity (Z_{dr}, dB) collected by the Polar55C radar, the algorithm described in [25] was applied to obtain the requested information on the ML (hereinafter $h_{0,R}$ and $\delta_{ML,R}$, where the subscript "*R*" stands for *radar*). As an example, Fig. 5 shows the time series of Z_h and Z_{dr} profiles collected during the precipitation event of 9 April 2018. In this case, the agreement between radar and NEFOCAST estimates of the ML bottom and top height is quite good, although a quite high temporal variability of both the ML height and thickness is observed. Moreover, the figure shows that the NEFOCAST model overestimates the height of the ML top in the first part of the event (before 13:00). Conversely, in the following part, the radar observed ML top height is greater and the ML is thinner than that assumed in the NEFOCAST algorithm. Considering all the available precipitation events observed by radar, the differences between h_0 used in the NEFOCAST algorithm and the one obtained from radar data are in most of the cases (i.e. 90%) less than 0.5 km, while the differences in terms of ML thickness are less than 50 m.

Knowing the disdrometer-measured DSDs for each precipitation event, rainfall rate (in mm h^{-1}) can be straightforwardly computed as

$$R_{TC} = 6\,\pi\,10^{-4} \int_{D_{min}}^{D_{max}} N(D)D^3\,v_t(D)\,dD \qquad (9)$$

where $v_t(D)$ is the particle terminal fall velocity [15] (in m s^{-1}), $N(D)$ is the drop size distribution (in m^{-3} mm^{-1}) while the diameter D is in mm. Then, the rain induced attenuation (L_{rain}) can be estimated through (8) considering the rainfall rate
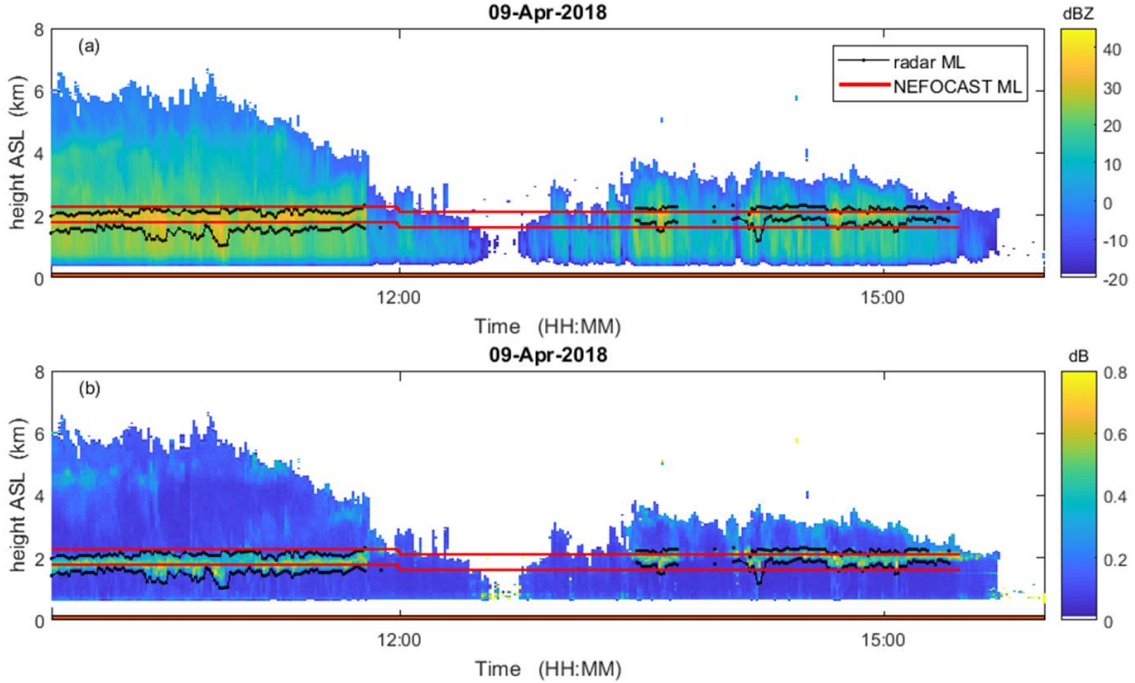

Fig. 5. Time series of (a) Z_h and (b) Z_{dr} collected by Polar 55C on 9 April 2018. Superimposed black lines represent the bottom and top of the ML as obtained from radar data by applying the algorithm described in **[25]**, while red lines represents the bottom and top of ML used in the NEFOCAST algorithm.

obtained from the measured DSD (9), the ML height and thickness both from the radar measured values (namely $h_{0,R}$ and $\delta_{ML,R}$) and from the values adopted in the NEFOCAST algorithm. We refer to $L_{rain,R}$ to indicate the rain induced attenuation obtained considering the values of ML height and thickness derived from radar data and to $L_{rain,N}$ to denote the rain induced attenuation obtained using the NEFOCAST algorithm. In order to evaluate the goodness of the agreement between $L_{rain,R}$ and $L_{rain,N}$, and consequently the error induced by the use of values of h_0 and δ_{ML} that differ from the actual ones, the Normalized Mean Absolute Error (NMAE), and the Root Mean Square Error (RMSE) were computed taking $L_{rain,R}$ as reference. Fig. 6a shows the scatterplot between $L_{rain,R}$ and $L_{rain,N}$ for all the selected rainfall events (2158 rain minutes in total). The agreement is good as highlighted by the low value of RMSE (RMSE = 0.06 dB), while NMAE = 21.3% indicates a not negligible amount of scattering

of the data, in particular for low attenuation values. **Please note that Fig. 6a presents two points with rain attenuation values greater that 1.85 dB that is the maximum measurable attenuation by SmartLNB. The latter is due to the fact the data shown in Fig. 6a were simulated from available disdrometer-measured rainfall rates that can be greater than the maximum rainfall rate retrievable from SmartLNB measurements. However, the obtained merit parameters indicated above do not change eliminating these two data point.** We can conclude that, for the adopted ML model, the use of model-predicted h_0 and δ_{ML} has a limited impact on total attenuation estimation.

The effect of ML geometry assumptions can be evaluated also in terms of rain rate. For this purpose, we compared the rainfall rate values obtained by inverting (8) with the h_0 and δ_{ML} adopted in the NEFOCAST algorithm using $L_{rain} = L_{rain,R}$ or $L_{rain} = L_{rain,N}$. Obviously, when $L_{rain} = L_{rain,N}$ the R from disdrometer DSD (namely R_{TC}) is obtained, while we refer to $R_{inv,R}$ when $L_{rain} = L_{rain,R}$. Fig. 6b shows the scatterplot between R_{TC} and $R_{inv,R}$. From the corresponding merit values (RMSE = 0.63 mm h^{-1} and NMAE = 19.2%), it can be concluded that there is a limited impact of the ML geometry model errors on the rainfall rate retrieved with the NEFOCAST algorithm.

B. Impact of k-R relations on the results

In the NEFOCAST algorithm, the *k-R* relation for liquid rain (i.e. α_{LL} and β_{LL} in (8)) was obtained experimentally from a long time series of disdrometer measured DSDs in Rome and is expected to be more representative of the climatology of the area of interest [13], [17], while the coefficients of the *k-R* relation within the ML (i.e. α_{ML} and β_{ML} in (8)) were taken from the literature. Microphysical and e.m. modelling of the ML are challenging research tasks. In [24] and [26] provided are two different sets of parameters to model the relation between specific attenuation and rainfall rate in the ML. The NEFOCAST algorithm adopts the model in [24], anyhow we tested both models finding a negligible difference (around 2%) for what concerns the ML attenuation estimate.
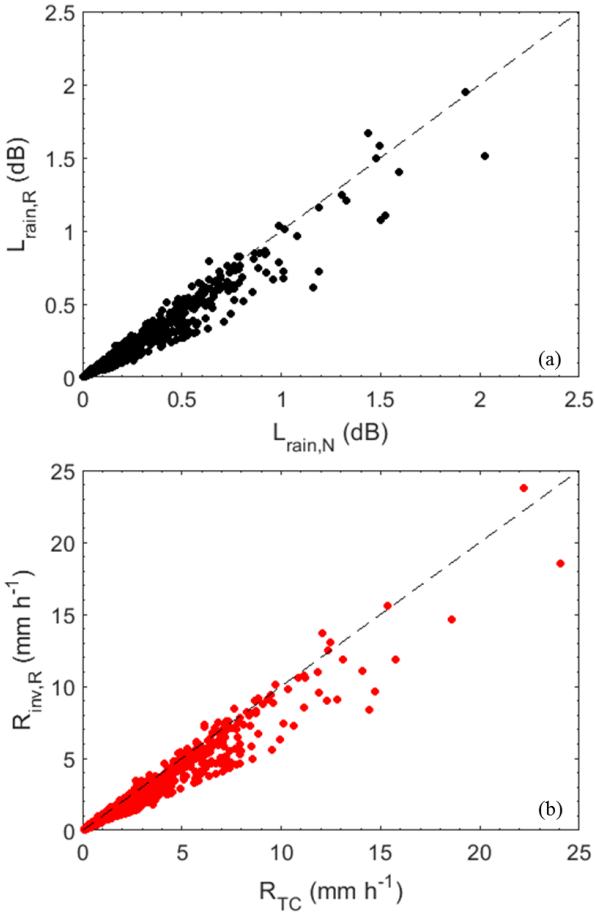
Fig. 6. Scatterplot between (a) $L_{rain,R}$ and $L_{rain,N}$ and (b) R_{TC} and $R_{inv,R}$

The focus of this section is on the quantitative evaluation of the impact of using a fixed a priori k-R relation for rain in NEFOCAST algorithm, with respect to DSD variability assuming as true the height and thickness of ML. The impact is evaluated in terms of both attenuation and rainfall rate estimates. Please notice, however, that the relevamt results have not generic validity, but they are specific for the NEFOCAST algorithm. In practice, for each disdrometer-measured DSD it is possible to obtain two different attenuation values: i) one from e.m. simulation applied to the measured DSD and, ii) one from applying the NEFOCAST algorithm to the rainfall rate associated to the same DSD.

i) Regarding the e.m. simulation, from a DSD the specific attenuation and the path integrated attenuation due to liquid rain (hereinafter $L_{rain,TM-LL}$ where the subscript "TM" stands for *T-matrix*) can be obtained as follows

$$L_{rain,TM-LL} = k\,(h_0 - \delta_{ML})/sin(\vartheta) \qquad (10)$$

$$k = C_k \int_{D_{min}}^{D_{max}} \sigma_E(p,\lambda,T,D)N(D)dD \qquad (11)$$

where σ_E is the extinction cross section that depends on the polarization (p is a label indicating polarization that can be either "vertical", "horizontal" or "circular"), on the wavelength of the incident wave, on the temperature (T) and on the hydrometeor diameter (D, mm), while C_k= 4.343 10^{-3}. In the present study, σ_E was computed using the T-matrix e.m. simulation model described in [27] with the following assumptions: incident wave frequency equal to 11.3458 GHz, environmental temperature equal to 20°C, Gaussian distribution of the canting angle with mean 0° and standard deviation 10°, drop shape following the model described in [28] and elevation angle θ_e=41.8°. Therefore $L_{rain,TM-LL}$ is only based on the extinction properties of the hydrometeors weighted for a given DSD, without referring to any specific *k-R* relation and assuming constant specific attenuation along the path.

ii) On the other hand, starting from a measured DSD, an estimate of the corresponding attenuation (hereinafter termed as $L_{rain,N-LL}$) can be obtained by resorting to (8), **considering only the contribution of LL with the same values of α_{LL}, β_{LL}, h_0 and δ_{ML} used in the NEFOCAST algorithm and assuming as the rain rate R_{LL} the value obtained from DSD data in** (9).
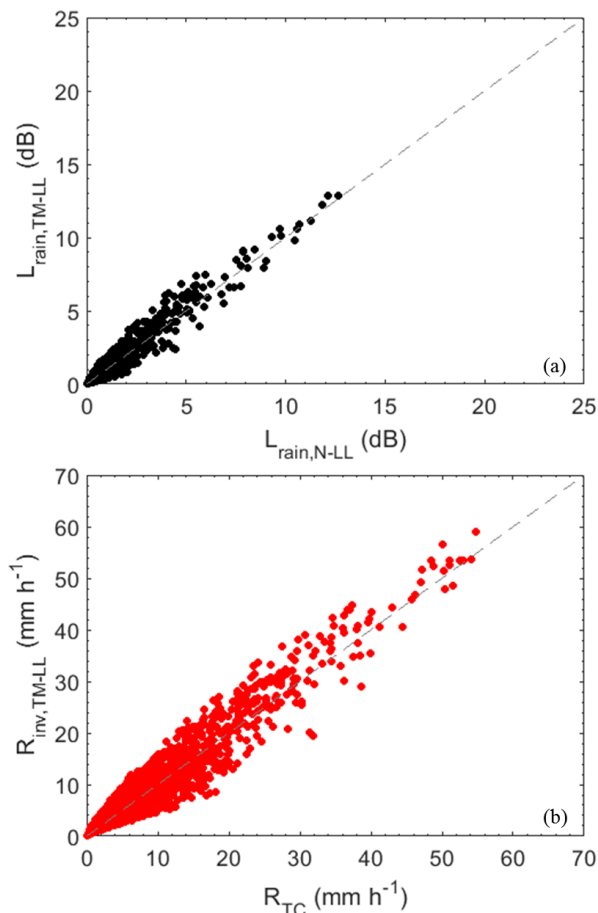

Fig. 7. Scatterplot between (a) $L_{rain,TM-LL}$ and $L_{ra,in,N-LL}$ and (b) R_{TC} and $R_{inv,TM-LL}$

The scatterplot between $L_{rain,TM-LL}$ and $L_{rain,N-LL}$ (Fig.7a) shows a good agreement between the two estimates, indicating a limited impact of using the *k-R* relation on the total attenuation. Please note that in Fig.7 the number of rainy minutes is higher (i.e. 21053 samples) than that in Figs 6 because we considered all the available disdrometer data and not only the ones coincident

with radar data. **The corresponding values of RMSE and NMAE are 0.12 dB and 25.5%, respectively. Similarly to Fig.6a, Fig.7a reports attenuations higher than 1.85 dB, i.e. the maximum attenuation measured by the SmartLNB. This happens only for the 2% of the datasets and furthermore the merit parameters do not change significantly considering only rain attenuation < 1.85 dB. (i.e. RMSE= 0.08 mm h^{-1} and NAME = 29.7%).** These results allow us to quantify the error induced by the use of the k-R relation on the attenuation estimates.

The latter can be evaluated also in terms of rain rate by inverting (8). As matter of fact, assuming in (8) α_{LL}, β_{LL}, h_0 and δ_{ML} as used in the NEFOCAST algorithm, and $L_{rain} = L_{rain,TM-LL}$ it is possible to obtain the corresponding rainfall rate that will be referred to as $R_{inv,TM-LL}$. **Instead, when $L_{rain} = L_{rain,N-LL}$, inverting (8) we take back the rainfall rate R_{TC} obtained from disdrometer data in (9).** In Fig.7b, $R_{inv,TM-LL}$ is compared with R_{TC} finding a small values of RMSE (i.e. RMSE = 0.90 mm h^{-1}), however a certain dispersion of the data is evident and leads to an NMAE = 21.5%. **Please note that considering only rain attenuation < 1.85 dB NMAE = 23.0% and RMSE = 0.75 mm h^{-1} are obtained.** The latter merit parameters identify the error (in terms of derived rain rate) due to the use of the k-R relation.

V. EVALUATION OF THE PRECIPITATION ESTIMATION FROM SMARTLNB

In this section, the rain gauge measurements and the SmartLNB estimates obtained from the VN set up in Tuscany are compared. In spite of their shortcomings, rain gauge measurements are traditionally considered as the "ground truth" for precipitation measurements. For a more in-depth analysis the SmartLNB estimates were also compared with the measurements obtained by the TC disdrometer in Rome. Notice that the rain gauge and the disdrometer provide a point measurement, while the SmartLNB provides an average precipitation along a path of a few kilometers. The latter difference in measuring area causes an underestimation of the precipitation peaks by the SmartLNB.

A. SmartLNB estimates vs rain gauge measurements

In this section, the precipitation measurements obtained from the SmartLNBs of the VN in the Florence area are compared with those provided by the co-located rain gauges. As shown in Section II, there are 6 sites with co-located SmartLNB and rain gauge. The comparison was made on an event basis. A rain event is considered to last at least 90 minutes with a maximum of 30 consecutive no-rain minutes. Furthermore, we discarded the events with rainfall amounts less than 1.5 mm. The selection of the rain events is driven by the rain gauge data.

All the rain gauge or SmartLNB rainy minutes between the beginning and the end of a given event have been considered to compute the total cumulated precipitation of that event. During the considered events the h_0 values range between 1.24 km and 3.92 km with a mean value of 2.12 km. In the following $R_{cum,G}$ and $R_{cum,S}$, (mm), denote the cumulated precipitation estimated by rain gauge and SmartLNB, respectively. Fig. 8 shows the scatterplot between $R_{cum,G}$ and $R_{cum,S}$ for the different sites. Shown are only the events with at least 30 minutes of coincident measurements. In the case of long lasting events, the SmartLNB seems to overestimate the cumulated precipitation with respect to the rain gauge, while the opposite holds for events that last one hour or less. The performance of the SmartLNB in estimating rainfall accumulation is illustrated in TABLE II through the values of RMSE, NMAE, and normalised bias (NB) between $R_{cum,G}$ and $R_{cum,S}$ obtained for each of the considered sites, as well as of RMSE, NMAE, and NB obtained considering the compete set of data from all the sites.

The NMAE (RMSE) values vary among the different sites ranging between 44.3% (5.25 mm) and 82.4% (11.54 mm) with an overall performance of 55.1% (7.58 mm). Based on NMAE, the SmartLNB identified as NEFOCAST-ITA-FI001S has the best performance, while the one with the lowest value of RMSE is the NEFOCAST-ITA-FI009S. In terms of bias, different behaviours are recorded. There are some sites with negative NB values and others with positive values (positive NBs indicate an overestimation of SmartLNB with respect to rain gauge). At some sites, such as NEFOCAST-ITA-FI001S and NEFOCAST-ITA-FI009S, the bias is negligible, while is high in NEFOCAST-ITA-FI010S. However, the overall bias is less than 20%.
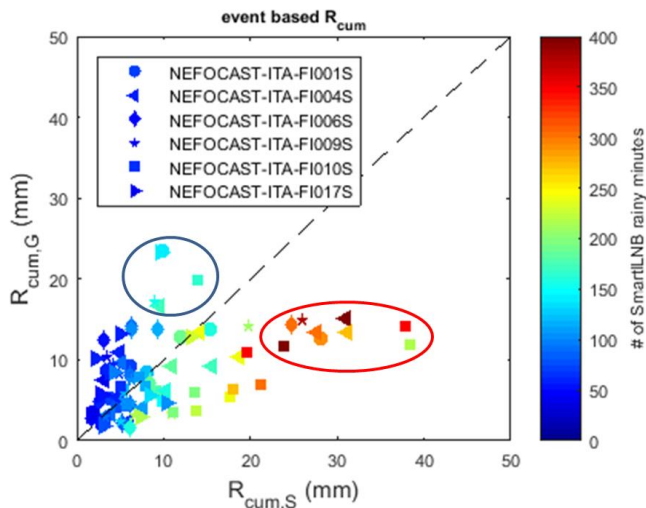
Fig. 8. Scatterplot between event-based cumulated precipitations estimated by SmartLNB (x-axis) and rain gauge (y-axis). The colorbar represents the number of rainy minutes collected by the SmartLNB during the event. Excessive overestimation and underestimation cases are circled with blue and red lines, respectively.

In spite of this good overall bias, data in Fig. 8 shows some dots evidencing a considerable over/under-estimation of SmartLNB with respect to rain gauge. Such outliers were analyzed separately. We verified that the dots corresponding to the higher underestimation of the SmartLNB with respect to rain gauge (those circled in blue in Fig. 8) correspond to the same rainy event, occurred on 29 October 2018. It was a mainly convective event with several peaks reaching even 70 mm h^{-1} (Fig. 9). The rain gauges recorded correctly the high precipitation rates, while the SmartLNBs tend to underestimate the precipitation peaks. As stated above, the latter is likely due to the different acquisition geometry; in fact, rain gauge provides a direct measurement referred to a point at surface level, while the SmartLNB technique, assumes a constant precipitation along the slant Earth-satellite path (that can be fews km long) and retrieves the rainfall rate from the path integrated attenuation value at disposal. As apparent, in some conditions, such as the one shown in Fig.9a around 05:00 UTC, the SmartLNB undergoes service outage due to very intense precipitation (up to 70 mm h^{-1} referring to rain gauge data) which causes a deep fade of the received SNR, well below η_{outage} (i.e., 5 dB). With the specific SmartLNBs used in this study, the upper rainfall rate limit that can be reached is between 30 mm h^{-1} and 16 mm h^{-1} , for 0° C isotherm ranging between 1 km and 2.5 km. It should be noted that this is the only outage situation in all the experimental field campaign. **Furthermore, we would like to stress that in heavy precipitation minutes, although the SmartLNB is not able provide precise quantitative measurements (as previously outlined in Section III-C), it is able to provide qualitative information (i.e. precipitation is present and takes a value greater than corresponding to the attenuation of η_{outage}) that can be used in a spatialization algorithm.**

TABLE II

PERFORMANCE OF THE SMARTLNB IN ESTIMATING RAINFALL ACCUMULATION WITH RESPECT TO RAIN GAUGE

Site name	RMSE (mm)	NMAE (%)	NB (%)
NEFOCAST-ITA-FI001S	6.07	44.3	-4.9
NEFOCAST-ITA-FI004S	7.82	48.1	34.9
NEFOCAST-ITA-FI006S	5.61	64.6	-13.7
NEFOCAST-ITA-FI009S	5.25	49.7	6.4
NEFOCAST-ITA-FI010S	11.54	56.0	99.7
NEFOCAST-ITA-FI017S	5.71	82.4	-31.0
All sites	7.58	55.1	19.3

Dots corresponding to a high overestimation of SmartLNB with respect to rain gauge (circled in red in Fig. 8), are from only 3
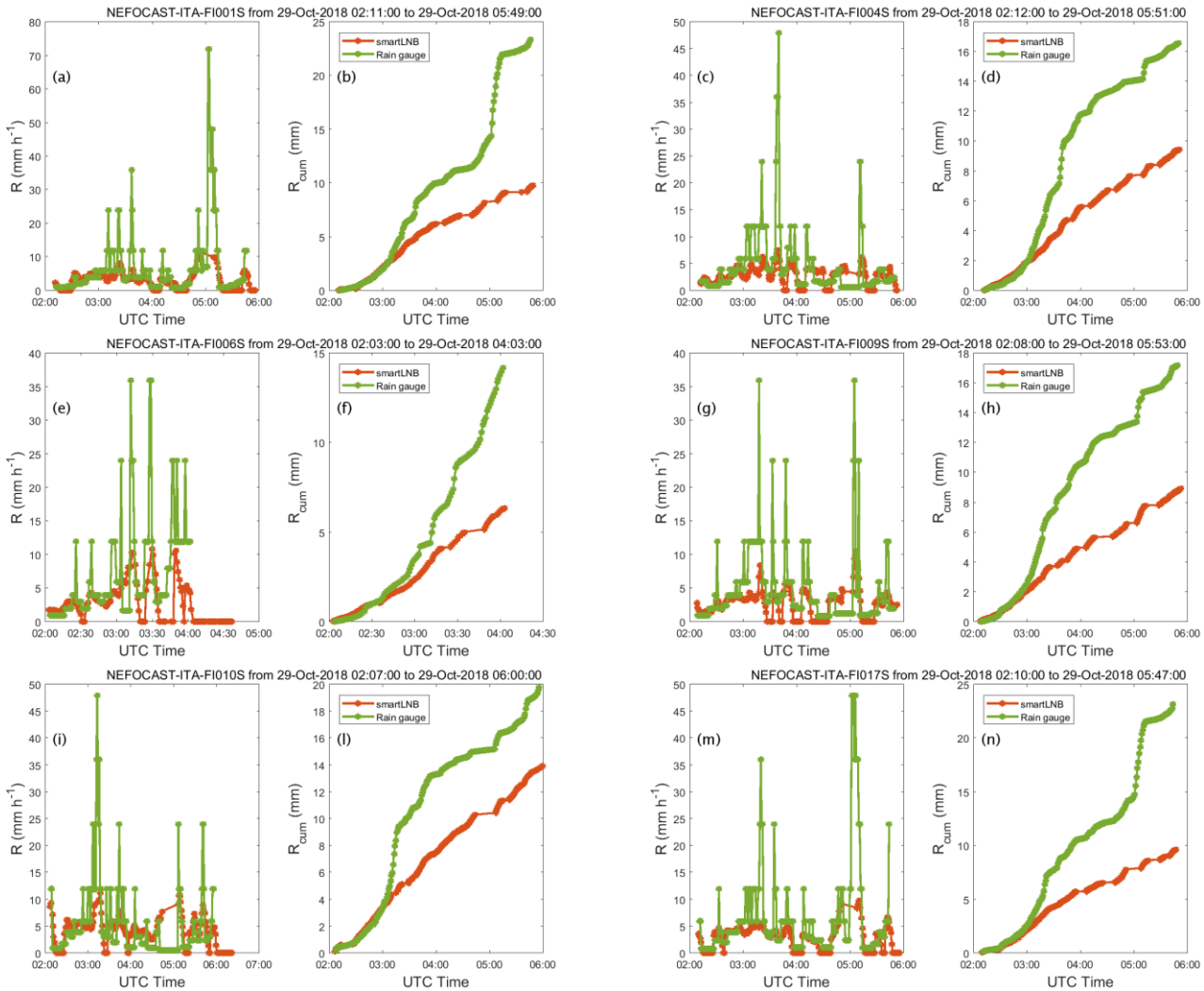

Fig. 9: Time series of R and R_{cum} derived from rain gauge and SmartLNB data collected at the six sites during the 29 October 2018 rain event.

events occurred on 2-3 December 2018, 16 December 2018, and 1-2 February 2019. Of these, the event of 16 December 2018 was the most peculiar. It was a stratiform event with long-lasting (roughly 6 hours) light precipitation (less than 10 mm h^{-1}) that hit all the 6 sites in the Florence area. At 5 sites, the SmartLNB highly overestimates the cumulated precipitation with respect to rain gauge, while at one site the agreement between the two devices is very good. As shown in Fig. 10a,c,e,g,i, although there is a good agreement between the trends of the two time series of instantaneous rainfall rate, there is also a small bias between the two estimates that causes SmartLNB overestimation. This bias is likely due to a failure of the NEFOCAST retrieval algorithm in determining the reference value of the satellite signal, probably as a consequence of some peculiar conditions of the previous sample times used to determine the reference value. The latter leads to a small overestimation of the instantaneous rain rate of few millimeters per hour, but due to the long duration of the event, the difference in terms of cumulated precipitation is high. On the other hand, the site NEFOCAST-ITA-FI017S shows a very good agreement between the two measurements (Fig. 10m,n). Further analysis with auxiliary data is needed in order to understand and improve the performance of the algorithm, although beyond the scope of this paper. It is useful to recall that, in terms of agreement between SmartLNB and rain gauge, those shown in Fig. 9 and Fig. 10 are the two worst rain events of the dataset, but they are useful for highlighting the two main shortcomings of the proposed technology.

B. SmartLNB estimates vs disdrometer measurements

In this section, we compare the SmartLNB rainfall retrievals with the data collected by the TC disdrometer in Rome. Disdrometers provide instantaneous (i.e., within a short time interval) rainfall rate with a better resolution with respect to rain gauges, which, in fact, measure time cumulated rainfall. During the considered events the h_0 values range between 1.32 km and 3.97 km with a mean value of 2.56 km.

In Fig. 11a the SmartLNB-based cumulated precipitation ($R_{cum,s}$) obtained in each event is compared with that obtained from the disdrometer ($R_{cum,TC}$). The events were selected based on the TC data: only the events with at least 30 minutes of coincident measurements are shown. The agreement between $R_{cum,s}$ and $R_{cum,TC}$ is good with a small bias of 5.8% and NMAE of 48.8%. Similarly to what reported in the previous section, the event that shows the highest overestimation of the SmartLNB retrieval with respect to the disdrometer measurements corresponds is a stratiform one which occurred on 13-14 December 2018 and is characterized by very long-lasting (more than 20 hours) light rain (R lower than 7 mm h^{-1}). In this case, the SmartLNB overestimates the instantaneous rain rate of a few millimeter per hour (i.e. 2 or 3 mm h^{-1}), but this leads to a great difference of the cumulated rainfall obtained from the two devices during the whole event. For this event, the mean rain rate obtained from SmartLNB data is 3.25 mm h^{-1}, while for the TC is 0.87 mm h^{-1}.

As proof of the above, observe Fig. 11b which compares the event mean rain rate obtained from the SmartLNB measurements with those computed from the disdrometer. There is an overall good agreement with a small overestimation of the SmartLNB (NB is equal to 13.2%), in particular for small mean rain rate values. The dark red dots, which correspond to long lasting events for which the total cumulated precipitation estimated from SmartLNB data is higher than that measured by rain gauge (Fig. 11a), in Fig. 11b indicate a good agreement in terms of average rain rate.
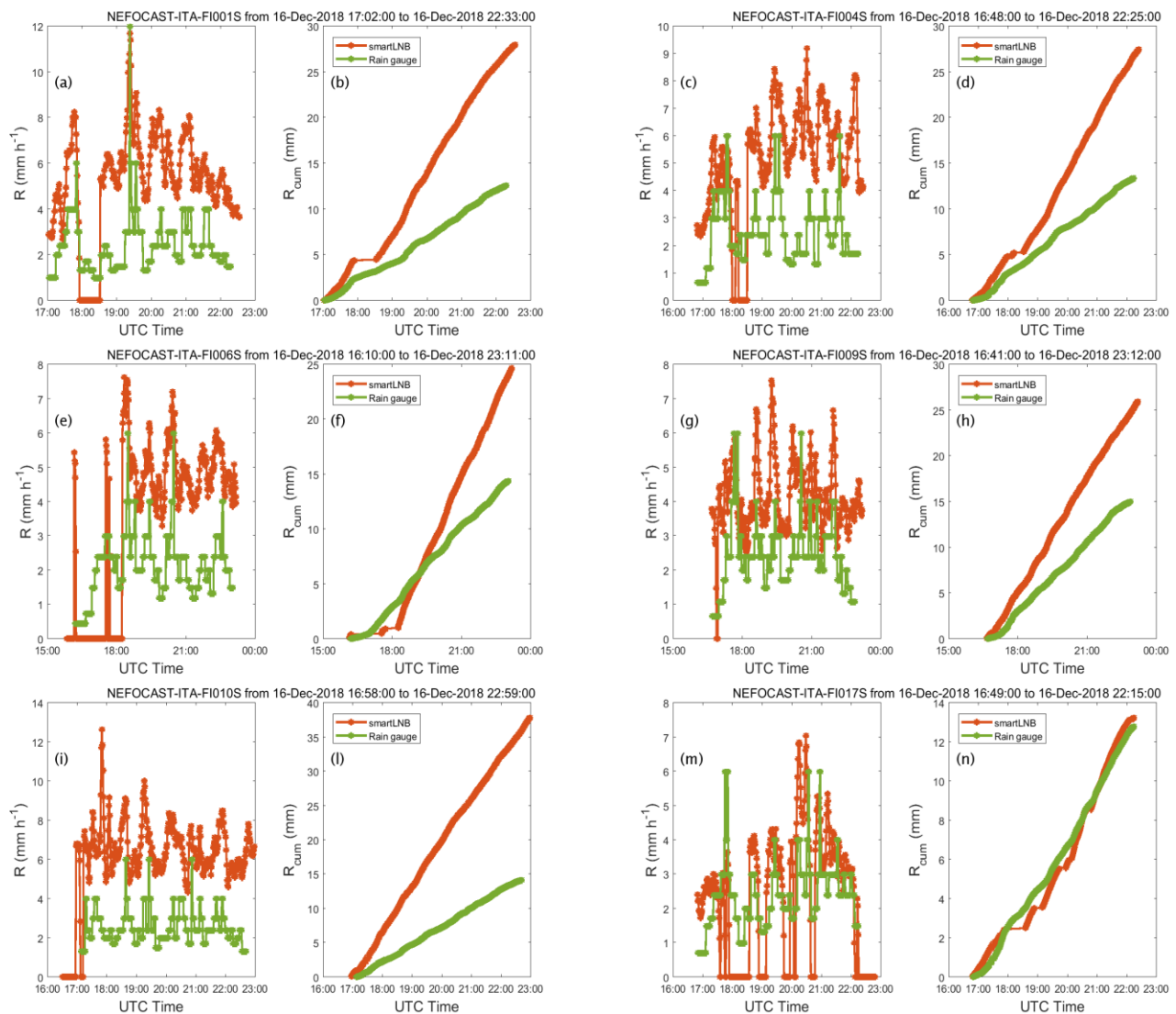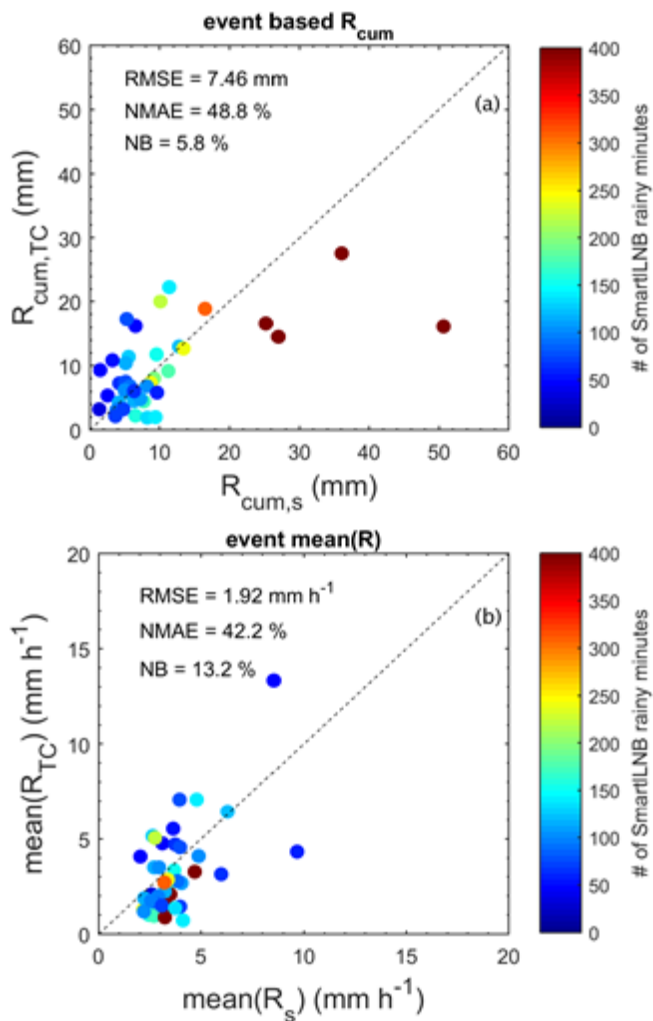

Fig. 10: As Fig. 9, for the 16 December 2018 rain event.

Fig. 11. (a) As Fig.8, with disdrometer data on y-axis. (b) Scatterplot between event mean rain rate obtained from SmartLNB (x-axis) and disdrometer (y-axis). The colorbar represents the number of rainy minutes collected by SmartLNB within the event.

VI. CONCLUSION

In the last decade, some studies have been presented illustrating how to exploit opportunistic signals of microwave Earth-space communication links in order to retrieve rainfall rate by measuring the attenuation experienced by the signals as a consequence of the presence of liquid and mixed precipitation along the receiver-satellite path. In this context, the 2-year NEFOCAST project (2017-2019) was conducted with the purpose to develop, tune, and test an *ad hoc* algorithm to retrieve precipitation rate from interactive domestic devices (the SmartLNBs), which are primarily used as digital broadcast TV receivers, but are able to measure and to relay SNR data on a continuous time basis. To keep the implementation as simple as possible the use of external data is limited to the height of 0°C that can be easily obtained from weather forecast models. First, thanks to coincident SmartLNB, disdrometer, and C-band radar data available on the roof of the ISAC-CNR building in Rome, intrinsic errors of the NEFOCAST algorithm were analyzed and quantified. In particular, we found a limited impact of both *i)* the k-R relation used to model attenuation in the liquid layer, and *ii)* the melting layer geometry information on the rainfall estimated by the SmartLNB (see section IV). ~~Specifically, the use of the melting layer thickness and height estimated from the radar measurements, instead of the ones obtained from the forecast model, provided RMSE = 0.63 mm h^{-1} and NMAE = 19.2% in terms of rainfall rate, while the impact of the k-R relation is a bit higher, with RMSE and NMAE of 0.90 mm h^{-1} and 21.5%, respectively. Furthermore, we found that the influence of the ML model adopted is very limited, with a difference in terms of total attenuation (L_{rain}) around 2% when the k-R coefficients of [26] are used instead of those proposed in [24].~~

In order to validate the rainfall rate estimated through the NEFOCAST algorithm, a 1-year field campaign was conducted in Tuscany. The analysis of the data collected during the campaign allowed us to assess the potential of the method, while the thorough analysis of the outliers helped us to identify the main shortcomings in the estimation of the rainfall rate. As remarked

before in Sect. III-C, the main limitation is the fact that, in the presence of very intense precipitation, the SmartLNB experiences service outage, which limits its measurement capability to rainfall intensities lower than 30 mm h^{-1} (for 0° isotherm height equal to 1 km). Such limit can be overcome with technological improvements aimed at providing receivers with higher rain fade margin (e.g., using larger parabolas), which entails a wider measurement dynamics.

By comparing, for each of the 6 sites of the VN, the total event cumulated precipitation measured by rain gauge with that estimated from the SmartLNB, we obtained values of NMAE (RMSE) between 44.3% and 82.4% (5.25 mm and 11.54 mm). In terms of bias, there are some sites where the SmartLNB overstimates the cumulated precipitation with respect to the rain gauge, while others show the opposite. However, considering all the SmartLNB and rain gauge data, a normalised bias of 19.3% is found.

Furthermore, at the Rome site the SmartLNB estimates were compared with the data collected by a disdrometer that is supposed to capture better the small temporal variations of rainfall because it provides one measurement per minute, while the rain gauge needs a minimum of 0.2 mm of cumulated precipitation to provide a single measurement. Comparing the disdrometer and SmartLNB event cumulated precipitation values, we obtained an NMAE (RMSE) equal to 48.8% (7.46 mm) and a small bias of 5.8%, while the comparison in terms of event mean rainfall rate reaches to a RMSE of 1.93 mm h^{-1} and a NB of 13.2%.

The results summarized above highlight the high potential of the proposed system to estimate precipitation. In densely popolated areas, a dense network of domestic receivers, as the SmartLNBs, has the potential to provide real-time accurate precipitation maps with high spatial and temporal resolution at practically no cost. On the other hand satellite interactive terminals (not necessarily those employed in this experiment) would provide a viable solution for obtaining precipitation data in regions of the Earth where rain measurements (i.e. rain gauge) are extremely scarce but DVB receivers could be available. In order to improve the proposed system, further investigation are needed, aimed for instance at improving the estimation of the dry baseline SNR in rainy conditions with the aim of improving the rainfall estimation in particular for light rain, at comparing areal precipitation estimations, at better estimating the attenuation effects of hydrometeors in mixing phase (such as the ones in the ML or during convective conditions), at evaluating the effect of precipitation inhomogeneity along the propagation path, and at investigating the possible synergies between SmartLNBs (or clusters of SmartLNBs), conventional meteorological devices and forecast models.

REFERENCES

[1] F. Y. Testik and M. Gebremichael, Rainfall: State of the Science, NJ, USA: John Wiley & Sons, Inc.: Hoboken, 2013.

[2] L. G. Lanza and E. Vuerich, "The WMO field intercomparison of rain intensity gauges," *Atmos. Res.,* vol. 94, no. 4, pp. 534-543, 2009.

[3] C. Kidd, A. Becker, G. Huffman, C. Muller, P. Joe, G. Skofronick-Jackson and D. Kirschbaum, "So, how much of the Earth's surface is covered by rain gauges?.," *Bull. Amer. Meteor. Soc.,* vol. 98, p. 69–78, 2017.

[4] G. Kathiravelu, T. Lucke and P. Nichols, "Rain drop measurement techniques: A Review," *Water,* vol. 8, p. 29, 2018.

[5] C. Andronache, Remote Sensing of Clouds and Precipitation., Springer, 2018.

[6] C. Kidd, A. Becker, G. J. Huffman, C. L. Muller, P. Joe, G. Skofronick-Jackson and D. B. Kirschbaum, "So, how much of the Earth's surface is covered by rain gauges?," *Bulletin of the American Meteorological Society,* vol. 98, no. 1, pp. 69-78, 2017.

[7] T. Oguchi, "Electromagnetic wave propagation and scattering in rain and other hydrometeors.," *Proc. IEEE,* vol. 71, p. 1029–1078, 1983.

[8] ITU, "Characteristics of precipitation for propagation modelling, Recommendation P.837-7," https://www.itu.int/rec/R-REC-P.837-7-201706-I/en, 2017.

[9] L. W. de Vos, A. Overeem, H. Leijnse and R. Uijlenhoet, "Rainfall Estimation Accuracy of a Nationwide Instantaneously Sampling Commercial Microwave Link Network: Error Dependency on Known Characteristics.," *J. Atmos. Oceanic Technol.,* vol. 36, p. 1267–1283, 2019.

[10] F. Barthès and C. Mallet, "Rainfall measurement from the opportunistic use of earth-space link in the Ku band," *Atmos. Meas. Tech.,* vol. 6, p. 2181–2193, 2013.

[11] C. H. Arslan, K. Aydin, J. V. Urbina and L. Dyrud, "Satellite-link attenuation measurement technique for estimating rainfall accumulation," *IEEE Trans Geosci Remote Sens,* vol. 56, no. 2, pp. 681-693, 2018.

[12] M. Colli, M. Stagnaro, A. Caridi, L. G. Lanza, A. Randazzo, M. Pastorino, D. D. Caviglia and A. Delicchi, "A field

assessment of a rain estimation system," *IEEE Trans Geosci Remote Sens,* vol. 57, no. 5, pp. 2864-2875, 2019.

[13]   F. Giannetti, R. Reggiannini, M. Moretti, E. Adirosi, L. Baldini, L. Facheris, A. Antonini, S. Melani, G. Bacci, A. Petrolino and A. Vaccaro, "Real-time rain rate evaluation via satellite downlink signal attenuation measurement.," *Sensors,* vol. 17, p. 1864, 2017.

[14]   F. Giannetti, R. Reggiannini, M. Moretti, S. Scarfone, A. Colicelli, F. Caparrini, G. Bacci, A. Petrolino, A. Vaccaro, E. Adirosi, A. Mazza and L. Facheris, "Kalman tracking of GEO satellite signal for opportunistic rain rate estimation," in *15th International Symposium on Wireless Communication Systems (ISWCS)*, Lisbon, Spain, 2018.

[15]   D. Atlas, R. Srivastava and R. Sekhon, " Doppler radar characteristics of precipitation at vertical incidence," *Rev. Geophys. Space Ge.,* vol. 11, pp. 1-35, 1973.

[16]   E. Adirosi, E. Volpi, F. Lombardo and L. Baldini, "Raindrop size distribution: Fitting performance of common theoretical models," *Adv. Water Resour,* vol. 96, pp. 290-305, 2016.

[17]   E. Adirosi, N. Roberto, M. Montopoli, E. Gorgucci and L. Baldini, "Influence of disdrometer type on weather radar algorithms from measured DSD: Application to Italian climatology," *Atmosphere,* vol. 9, no. 9, p. 360, 2018.

[18]   M. Montopoli, N. Roberto, E. Adirosi, E. Gorgucci and L. Baldini, "Investigation of weather radar quantitative precipitation estimation methodologies in complex orography," *Atmosphere,* vol. 8, no. 2, p. 34, 2017.

[19]   M. Alvarez-Diaz, R. Lopez-Valcarce and C. Mosquera, "SNR Estimation with Heterogeneous Frames," in *4th Advanced Satellite Mobile Systems*, Bologna, Italy., 2008 .

[20]   ETSI, "Digital Video Broadcasting (DVB); Second generation framing structure, channel coding and modulation systems for Broadcasting, Interactive Services, News Gathering and other broadband satellite applications; Part 1: DVB-S2, standard EN 302 307-1 V1".

[21]   ITU, "Attenuation by atmospheric gases. Recommendation ITU-R P.676-9," 02/2012.

[22]   ITU, "Attenuation due to clouds and fog. Reccomendation ITU-R P.840-8," 08/2019.

[23]   F. Giannetti, M. Moretti, R. Reggiannini and A. Vaccaro, "The NEFOCAST system for detection and estimation of rainfall fields by the opportunistic use of broadcast satellite signals," *IEEE Aerospace and Electronic Systems Magazine,* vol. 34, no. 6, pp. 16-27, 2019.

[24]   A. Dissanayake and N. McEwan, "Radar and attenuation properties of rain and bright band," in *International Conference on Antennas and Propagation*, London, England, 1978.

[25]   L. Baldini and E. Gorgucci, "Identification of the melting layer through dual-polarization radar measurements at vertical incidence," *J. Atmos. Oceanic Tech.,* vol. 23, pp. 829-839, 2006.

[26]   S. Y. Matrosov, "Assessment of Radar Signal Attenuation Caused," *IEEE TRANSACTIONS ON GEOSCIENCE AND REMOTE SENSING,* vol. 46, no. 4, pp. 1039-1047, 2008.

[27]   P.-W. Barber and C. Yen, "Scattering of electromagnetic waves by arbitrarily shaped dielectric bodies," *Appl. Opt.,* vol. 14, p. 2864–2872, 1975.

[28]   K. V. Beard and C. Chuang, "A new model for the equilibrium shape of raindrops," *J.Atmos. Sci.,* vol. 44, pp. 1509-1524, 1987.

Elisa Adirosi received the Master's degree in environmental engineering and the Ph.D. degree in environmental and hydraulic engineering from Sapienza University of Rome, Rome, Italy, 2009 and 2015, respectively. She has been Visiting Scientist at Goddard Space Flight Center, NASA, Greenbelt, MD, USA, and is currently a Researcher with the CNR-ISAC, Rome, Italy. She develops innovative mathematical methods to analyze disdrometer data, and investigates the characteristics of simulated and observed drop size distributions to improve precipitation retrieval from remote sensing measurements. She has been involved in NEFOCAST project.

Luca Facheris received the Laurea degree (cum laude) in electronic engineering and the Ph.D. degree in information engineering from the University of Padova, Italy, in 1989 and 1993, respectively.
From 1993 to 2002, he was an Assistant Professor with the Department of Information Engineering, University of Florence, where he has been an Associate Professor since 2002. His research interests include radar and active atmospheric remote sensing and definition of methods for the exploitation of attenuation measurements at microwaves and infrared for the remote sensing of rainfall, pollutants, and tropospheric water vapor. He has been involved in the NEFOCAST project

Filippo Giannetti received the Laurea and the Ph.D. degree in electronic engineering from the University of Pisa, Italy, in 1989 and from the University of Padova, Italy, in 1993, respectively. In 1988/89, he spent a research period at TELETTRA (now ALCATEL), in Vimercate, Milan, Italy, working on SONET/SDH radio modems. In 1992 he spent a research period at the European Space Agency Research and Technology Centre (ESA/ESTEC), Noordwijk, The Netherlands, where he was engaged in several activities in the field of digital satellite communications. Since 1993 he has been with the Department of Information Engineering of the University of Pisa, where he is currently Associate Professor of Telecommunications. His main research interests are in the broad area of wireless terrestrial and satellite communications, with special attention to digital modulations, error-correcting codes, multiple-access techniques, digital modem architecture design, radio resource allocation, signal processing for communications, radio propagation, and radiolocation techniques. He is the author of more than 150 journal and conference papers and co-inventor of several patents, jointly developed with ESA. He is also member of the editorial board of EURASIP Journal on Wireless Communications and Networking. He has been involved in NEFOCAST project.

Simone Scarfone received the master's degree in telecommunications engineering from the University of Pisa, Pisa, Italy, in 2016. From 2016 to 2018, he has been a research fellow at the Department of Information Engineering (DII) of the University of Pisa where he was involved in the evaluation of satellite link-budgets and in the development of signal processing algorithms in the framework of the Nefocast project. Currently, he is a PhD student at DII, working on radio-resource allocation algorithms for V2X communications within H2020 EPI project. He has been involved in NEFOCAST project.

Giacomo Bacci (S'07–M'09) received the B.E. and the M.E. degrees in telecommunications engineering and the Ph.D. degree in information engineering from the University of Pisa, Pisa, Italy, in 2002, 2004, and 2008, respectively. In 2006-07, he was a visiting student research collaborator at Princeton University, Princeton, NJ, USA. In 2008-14, he was a post-doctoral research fellow at the University of Pisa. In 2008-2012, he also joined Wiser srl, Livorno, Italy, as a software engineer, and in 2012-14 he was also enrolled as a visiting postdoctoral research associate at Princeton University. Since 2015, he has joined MBI srl, Pisa, Italy, as a product manager for interactive satellite broadband communications. Dr. Bacci is the recipient of the FP7 Marie Curie International Outgoing Fellowships for career development (IOF) 2011 GRAND-CRU, and received the Best Paper Award from the IEEE Wireless Commun. and Networking Conference (WCNC) 2013, the Best Student Paper Award from the Intl. Waveform Diversity and Design Conf. (WDD) 2007, and the Best Session Paper at the ESA Workshop on EGNOS Performance and Applications 2005. He is also the recipient of the 2014 URSI Young Scientist Award, and he has been named an Exemplary Reviewer 2012 for IEEE Wireless Communications Letters. He has been involved in NEFOCAST project.

Alessandro Mazza received his master's degree in physics at the University of Florence in 1992. In 1998, he obtained his PhD in physics at the University of Pisa with a thesis on quantum mechanics. From 1992 to 1994, he worked for the SMA company. Since 2001, he has worked at LAMMA first in the Information Technology group then in the atmospheric research division. Since 2012, he has worked on radar meteorology applications and hydrology. Since 2003, he has been a researcher at CNR-IBIMET institute. He has been involved in NEFOCAST project.

Alberto Ortolani received the Master's degree in physics (cum laude) from University of Florence, Florence, Italy, and the Ph.D. degree in physical modeling for environmental protection from the University of Bologna, Bologna, Italy. In 1996 he had temporary contracts to work on X-ray stellar spectroscopy with the Palermo Astronomical Observatory. In 1997-1998 he worked for the SMA company (Systems for the meteorology and the environment) in Florence on satellite SAR imagery. In 1997 he won a three-year Marie Curie grant to work on astrophysics, then declined to continue the career on remote sensing. From 1998 to 2002 he worked for FCS (Foundation for the climate and the sustainability) of Florence on remote sensing applications to the sea and the atmosphere. Since 2002 he has joined the Italian National Research Council, Institute for the Bioeconomy (former Institute for the Biometeorology) where presently he is senior researcher. Since 1997 the working activities have been developed in the framework of Consorzio LaMMA (former LaMMA project) where now he is assigned by CNR and he is head of the atmospheric research division, focused on project developments in satellite, radar and GNSS meteorology, atmospheric modeling and data assimilation, meteo-based services for maritime transportation. Since 2015 he is CNR representative in the Tuscany industrial district of yachting and ports. Since 2018 he teaches "Physics of the atmosphere" at the Master degree in Physical and Astrophysical Sciences of the University of Florence. He has been involved in NEFOCAST project.

Luca Baldini (M'95–SM'08) received the Laurea degree in electrical engineering and the Ph.D. degree in methods and technologies for environmental monitoring from the University of Florence, Florence, Italy, in 1988 and 1994 respectively. From 1991 to 1994, he was Assistant Teacher with the University of Florence, of "Theory and Radar Techniques." From 1994 to 2001, he was a Teacher with the University of Siena, Sienna, Italy, in "Remote Sensing Systems" and with the University of Florence in "Signal Theory," in 1996. From 1995 to 2001, he was a consultant in Italy. In 2001, he joined as Researcher with the CNR-ISAC, Rome, Italy, where he is in charge of research on radar polarimetry applied to rainfall estimation, characterization of precipitation microphysics, and ground validation of precipitation measurements from satellites. He has been involved in NEFOCAST project.